

Direct Detection of Dark Matter in Supersymmetric Models

Howard Baer, Csaba Balázs, Alexander Belyaev* and Jorge O’Farrill

Department of Physics, Florida State University Tallahassee, FL 32306, USA

*E-mail: baer@hep.fsu.edu, balazs@hep.fsu.edu, belyaev@hep.fsu.edu,
ofarrill@hep.fsu.edu*

ABSTRACT: We evaluate neutralino-nucleon scattering rates in several well-motivated supersymmetric models, and compare against constraints on the neutralino relic density, $BF(b \rightarrow s\gamma)$ as well as the muon anomalous magnetic moment a_μ . In the mSUGRA model, the indirect constraints favor the hyperbolic branch/focus point (HB/FP) region of parameter space, and in fact this region is just where neutralino-nucleon scattering rates are high enough to be detected in direct dark matter search experiments! In Yukawa unified SUSY $SO(10)$ models with scalar mass non-universality, the relic density of neutralinos is almost always above experimental bounds, while the corresponding direct detection rates are below experimental levels. Conversely, in five dimensional $SO(10)$ models where gauge symmetry breaking is the result of compactification of the extra dimension, and supersymmetry breaking is communicated via gaugino mediation, the relic density is quite low, while direct detection rates can be substantial.

KEYWORDS: Supersymmetry Phenomenology, Supersymmetric Standard Model, Dark Matter.

*On leave of absence from Nuclear Physics Institute, Moscow State University.

1. Introduction

A wide variety of astrophysical data now point conclusively to the existence of cold dark matter (CDM) in the universe. The most recent results come from the Wilkinson Microwave Anisotropy Probe (WMAP)[1]. Their results confirm the standard model of cosmology and fit its parameters to high precision. The properties of a flat universe in the Λ CDM model are characterized by the density of baryons (Ω_b), matter density (Ω_m), vacuum energy (Ω_Λ) and the expansion rate (h) which are measured to be:

$$\Omega_b = 0.044 \pm 0.004 \tag{1.1}$$

$$\Omega_m = 0.27 \pm 0.04 \tag{1.2}$$

$$\Omega_\Lambda = 0.73 \pm 0.04 \tag{1.3}$$

$$h = 0.71^{+0.04}_{-0.03}. \tag{1.4}$$

From the WMAP results one derives the following value for the cold dark matter density:

$$\Omega_{CDM}h^2 = 0.1126^{+0.0081}_{-0.0090} \left({}^{+0.0161}_{-0.0181} \right) \text{ at } 68(95)\% \text{ CL.} \tag{1.5}$$

In spite of the excellent fit to the data, the standard cosmological model has several fundamental open questions. One of these is the origin and nature of dark matter. Within the context of R -parity conserving supersymmetry (SUSY) [2] the lightest supersymmetric particle (LSP) offers a robust solution to this problem. First, SUSY itself is the most complete theoretical extension of the Standard Model (SM), and is well motivated experimentally. This solidly supports the neutralino LSP dark matter theoretically. Second, the WMAP results strongly restrict neutrino hot dark matter to $\Omega_\nu h^2 < 0.0076$ (95%CL) and also exclude warm dark matter based on detection of re-ionization at $z \sim 20$. Warm dark matter in the form of gravitinos could also be a good candidate for dark matter in certain supersymmetric models, but WMAP has vetoed this option. Therefore, in the light of recent WMAP results, the neutralino LSP emerges as one of the most attractive candidate for CDM.

If indeed all space is filled with relic neutralinos, then it may be possible to directly detect them via their scattering from nuclei, or to indirectly detect them via their annihilation products. There are two kinds of non-accelerator experiments aimed at the CDM search. One way is to search for the products of neutralino annihilation in outer space or inside the sun or earth where they become concentrated due to the gravitational force. Another way to search for CDM is via direct detection from their scattering off nuclei by measuring the nuclear recoil. There are several existing and future projects engaged in the direct search for weakly interacting massive particles (WIMPs) [3]. These include experiments based on germanium detectors such as IGEX [4], HDMS [5], CDMS [6], EDELWEISS [7] and GENIUS [8]. Scintillator detectors are used by DAMA [9] and ZEPLIN [10, 11, 12, 13]. Projection chambers utilized in DRIFT [14], and metastable particle detectors in SIMPLE [15] and PICASSO [16].

Presently the best limits on the spin-independent WIMP-nucleon cross-section (σ_{SI}) have been obtained by the CDMS, EDELWEISS and ZEPLIN1 groups, while a signal is

claimed by the DAMA collaboration. Collectively, we will refer to the reach from these groups as the “Stage 1” dark matter search. Depending on the neutralino mass, the combined limit on the neutralino-proton spin-independent cross section σ_{SI} varies from 10^{-5} to 10^{-6} pb. This cross section range is beyond the predicted levels from most supersymmetric models if one also requires the model to be within the experimental constraints from LEP2, $(g-2)_\mu$, $BF(b \rightarrow s\gamma)$, relic density $\Omega_{CDM}h^2$ and $BF(B_s \rightarrow \mu^+\mu^-)$ data. However, experiments in the near future like CDMS2, CRESST2, ZEPLIN2 and EDELWEISS2 (Stage 2 detectors) should have a reach of the order of 10^{-8} pb. Finally, a number of experiments such as GENIUS, ZEPLIN4 and CRYOARRAY are in the planning stage. We refer to them as Stage 3 detectors, which promise strong limits of the order of $\sigma_{SI} < 10^{-9} - 10^{-10}$ pb, and would allow the exploration of a considerable part of parameter space of many supersymmetric models.

Beginning with the paper by Goodman and Witten [17], there have been numerous studies on neutralino nuclei scattering rate evaluation [18, 19, 20, 21, 22, 23], with the trend of gradually improving the quality of calculations and extending the range of supersymmetric models. It is useful to note that in the case of the general MSSM, σ_{SI} could be several orders of magnitude higher [23] than in more constrained models such as the minimal supergravity model (mSUGRA).

In this paper, we perform an updated analysis of neutralino elastic scattering off nuclei in a class of supersymmetric models. There are various motivations for this study.

- We have included constraints from the neutralino relic density $\Omega_{\tilde{Z}_1} h^2$, the rare decays $b \rightarrow s\gamma$ and $B_s \rightarrow \mu^+\mu^-$, the muon anomalous magnetic moment a_μ , as well as from the LEP2 experiment. Together these constraints significantly restrict the SUSY model parameter space in the relevant range of σ_{SI} .
- We are using a new version of ISAJET, version 7.65[24], in which the complete one-loop corrections to sfermion masses [25] have been incorporated. In addition, the stability of the new version has been greatly improved in the low $|\mu|$ region which allows us to better access the hyperbolic branch/focus point (HB/FP) region of the mSUGRA model. This is important, because the HB/FP region can simultaneously satisfy constraints from $\Omega_{\tilde{Z}_1} h^2$, $(g-2)_\mu$, and $BF(b \rightarrow s\gamma)$ while offering a decoupling solution to the SUSY flavor and CP problems, and maintaining naturalness[26, 27, 28].
- Besides the mSUGRA model, we also analyse SUSY grand unified theories (GUTs) based on the $SO(10)$ group [29] where the MSSM Higgs doublets are both present in the same 10-dimensional Higgs multiplet. These models predict unification of the Yukawa couplings for the third generation: $f_t = f_b = f_\tau$. Following the strategy of our previous study [30], we examined models with a high degree of Yukawa coupling unification, and have evaluated neutralino nuclei scattering rates together with experimental constraints. For Yukawa unified models with $\mu < 0$, there exist parameter choices consistent with neutralino relic density constraints, although direct detection rates are frequently quite low. For models with $\mu > 0$, the relic density is almost

always above measured limits, while direct detection rates are almost always below experimentally accessible levels.

- We also examine an $SO(10)$ motivated SUSY GUT model [31] with non-universal gaugino masses and otherwise vanishing soft-parameters at the GUT scale. This setup is well motivated by SUSY GUTs constructed in higher dimensions [32, 33] utilizing gaugino mediated SUSY breaking. Many of these models elegantly solve the doublet-triplet splitting and fast proton decay problems of 4D SUSYGUT models [34] by the orbifold compactification of the extra dimensions. In the phenomenologically viable region of the parameter space of this model the lightest neutralino generally has a large higgsino or wino component, which leads to low values of $\Omega_{\tilde{Z}_1} h^2$, and neutralino dark matter would need to be augmented by other forms of CDM, such as axions, or hidden sector states. We find that σ_{SI} can frequently be several orders of magnitude larger than the mSUGRA case, owing to the large wino and/or higgsino component of the neutralino.

The rest of this paper is organized as follows. In Section 2 we discuss details of our evaluation of the neutralino-nucleon elastic scattering cross section. In Section 3, we present results for the mSUGRA model, and point out the intriguing features endemic to the HB/FP region. In Section 4, we perform studies for $SO(10)$ motivated Yukawa unified SUSY GUT models, while Section 5 presents results for SUSY GUT models with non-universal gaugino masses. In Section 6 we present our conclusions.

2. Details of calculation for neutralino elastic scattering on nuclei

The interactions for elastic scattering of neutralinos on nuclei can be described by the sum of spin-independent ($\mathcal{L}_{scalar}^{eff}$) and spin-dependent (\mathcal{L}_{spin}^{eff}) Lagrangian terms:

$$\mathcal{L}_{elastic}^{eff} = \mathcal{L}_{scalar}^{eff} + \mathcal{L}_{spin}^{eff}. \quad (2.1)$$

In this paper we evaluate the spin-independent cross section σ_{SI} of neutralino scattering off of nuclei which is the main experimental observable since σ_{SI} contributions from individual nucleons in the nucleus add coherently and can be expressed via SI nuclear form-factors. The cross section σ_{SI} receives contributions from neutralino-quark interactions via squark, Z and Higgs boson exchanges, and from neutralino-gluon interactions involving quarks, squarks and Higgs bosons at the 1-loop level. The differential σ_{SI} off a nucleus X_Z^A with mass m_A takes the form [35]

$$\frac{d\sigma^{SI}}{d|\vec{q}|^2} = \frac{1}{\pi v^2} [Z f_p + (A - Z) f_n]^2 F^2(Q_r), \quad (2.2)$$

where $\vec{q} = \frac{m_A m_{\tilde{Z}_1}}{m_A + m_{\tilde{Z}_1}} \vec{v}$ is the three-momentum transfer, $Q_r = \frac{|\vec{q}|^2}{2m_A}$ and $F^2(Q_r)$ is the scalar nuclear form factor, \vec{v} is the velocity of the incident neutralino and f_p and f_n are effective neutralino couplings to protons and neutrons respectively. This formalism has been

reviewed in [35, 19, 20]. Explicit expressions for f_p and f_n can be found, *e.g.* in [20]. The original calculation has been done in [19] and can be expressed as

$$\frac{f_N}{m_N} = \sum_{q=u,d,s} \frac{f_{Tq}^{(N)}}{m_q} \left[f_q^{(\tilde{q})} + f_q^{(H)} - \frac{1}{2} m_q m_{\tilde{Z}_1} g_q \right] + \frac{2}{27} f_{TG}^{(N)} \sum_{c,b,t} \frac{f_q^{(H)}}{m_q} + \dots \quad (2.3)$$

where $N = p, n$ for neutron, proton respectively, and $f_{TG}^{(N)} = 1 - \sum_{q=u,d,s} f_{Tq}^{(N)}$. The expressions for the $f_q^{(H)}$ couplings as well as other terms denoted by \dots are omitted for the sake of brevity but can be found in [19, 20].

The parameters $f_{Tq}^{(p)}$, defined by

$$\langle N | m_q \bar{q} q | N \rangle = m_N f_{Tq}^{(N)} \quad (q = u, d, s) \quad (2.4)$$

contains uncertainties due to errors on the experimental measurements of quark masses. We have adopted values of renormalization-invariant constants $f_{Tq}^{(p)}$ and their uncertainties determined in [21]

$$f_{Tu}^{(p)} = 0.020 \pm 0.004, \quad f_{Td}^{(p)} = 0.026 \pm 0.005, \quad f_{Ts}^{(p)} = 0.118 \pm 0.062 \quad (2.5)$$

$$f_{Tu}^{(n)} = 0.014 \pm 0.003, \quad f_{Td}^{(n)} = 0.036 \pm 0.008, \quad f_{Ts}^{(n)} = 0.118 \pm 0.062. \quad (2.6)$$

In this paper we calculate the quantity which is being conventionally used to compare experimental and theoretical results – the cross section σ_p^{SI} for neutralino scattering off the proton in the limit of zero momentum transfer

$$\sigma^{SI} = \frac{4}{\pi} m_r^{N^2} f_N^2 \quad (2.7)$$

where $m_r^N = m_N m_{\tilde{Z}_1} / (m_N + m_{\tilde{Z}_1})$.

In our calculations we have used the CTEQ5L set of parton density functions [36] evaluated at the QCD scale $Q = \sqrt{M_{SUSY}^2 - m_{\tilde{Z}_1}^2}$.

3. Direct detection rates in the mSUGRA model

We start with the analysis of the neutralino scattering rates in the minimal supergravity model [37]. The mSUGRA model assumes universal boundary conditions at the GUT scale for scalar and gaugino masses as well as for trilinear A -parameters and therefore is defined by a set of just four parameters and a sign:

$$m_0, m_{1/2}, A_0, \tan \beta \text{ and } \text{sign}(\mu), \quad (3.1)$$

where $\tan \beta = v_u/v_d$ parametrizes the Higgs sector. The top-quark pole mass is taken to be $m_t = 175$ GeV.

3.1 Experimental constraints

Before presenting results we discuss the following experimental constraints on the mSUGRA model.

- LEP2 constraints.** Based on negative searches for superpartners at LEP2 [38, 39], we require $m_{\tilde{W}_1} > 103.5$ GeV and $m_{\tilde{e}_{L,R}} > 99$ GeV provided $m_{\tilde{e}} - m_{\tilde{Z}_1} > 10$ GeV [38], which is the most stringent of the slepton mass limits. The LEP2 experiments also set a limit on the SM Higgs boson mass: $m_{H_{SM}} > 114.1$ GeV [40]. This is of relevance since in our mSUGRA parameter space scans, the lightest SUSY Higgs boson h is almost always SM-like.
- Neutralino relic density.** The WMAP results [1] set a stringent bound on the neutralino relic density, given by $0.0945 < \Omega_{CDM} h^2 < 0.129$ at 95% CL. The upper limit above represents a true constraint, while the corresponding lower limit is flexible, since there may be additional sources of CDM such as axions, or states associated with the hidden sector and/or extra dimensions. To estimate the relic density of neutralinos in the mSUGRA model, we use the recent calculation in Ref. [41]. In that work, all relevant neutralino annihilation and co-annihilation reactions are evaluated at tree level using the CompHEP [42] program. The annihilation cross section times velocity is relativistically thermally averaged [43], which is important for obtaining the correct neutralino relic density in the vicinity of annihilations through s -channel resonances.
- $b \rightarrow s\gamma$ decay.** The branching fraction $BF(b \rightarrow s\gamma)$ has been measured by the BELLE [44], CLEO [45] and ALEPH [46] collaborations. A weighted averaging of results yields $BF(b \rightarrow s\gamma) = (3.25 \pm 0.37) \times 10^{-4}$ at 95% CL. To this we should add uncertainty in the theoretical evaluation, which within the SM dominantly comes from the scale uncertainty, and is about 10%. Together, these imply the bounds, $2.16 \times 10^{-4} < BF(b \rightarrow s\gamma) < 4.34 \times 10^{-4}$. In our study, we show contours of $BF(b \rightarrow s\gamma)$ allowing the reader to decide the extent to which parameter space is excluded [47]. The calculation of $BF(b \rightarrow s\gamma)$ used here is based upon the program of Ref. [48]. Our value of the SM $b \rightarrow s\gamma$ branching fraction yields 3.4×10^{-4} , with a scale uncertainty of 10%.
- Muon anomalous magnetic moment.** The muon anomalous magnetic moment $a_\mu = (g - 2)_\mu / 2$ has been measured to high precision by the E821 experiment [49]. Comparison of the measured value against theoretical predictions gives, according to Hagiwara *et al.* [50]: $11.5 < \delta a_\mu \times 10^{10} < 60.7$. A different assessment of the theoretical uncertainties [50] using the procedure described in Ref. [47] gives, $-16.7 < \delta a_\mu \times 10^{10} < 49.1$. In view of the theoretical uncertainty, we only present contours of δa_μ , as calculated using the program developed in [51], and leave it to the reader to decide the extent of the parameter region allowed by the data.
- $B_s \rightarrow \mu^+ \mu^-$ decay.** The branching fraction of B_s to a pair of muons has been experimentally bounded by CDF [52]: $BF(B_s \rightarrow \mu^+ \mu^-) < 2.6 \times 10^{-6}$. While this

branching fraction is very small within the SM ($BF_{SM}(B_s \rightarrow \mu^+\mu^-) \simeq 3.4 \times 10^{-9}$), the amplitude for the Higgs-mediated decay of B_s grows as $\tan^3 \beta$ within the SUSY framework, and hence can completely dominate the SM contribution if $\tan \beta$ is large. In our analysis we use the results from [53] to delineate the region of mSUGRA parameters excluded by the CDF upper limit on its branching fraction.

3.2 mSUGRA results

In Fig. 1, we show our first results of the spin independent neutralino-nucleon elastic scattering cross section in the m_0 vs. $m_{1/2}$ parameter plane for $\tan \beta = 10 - 55$, with $A_0 = 0$ and for $\mu < 0$ (upper two rows) and $\mu > 0$ (lower two rows).

In this figure we have applied only LEP2 constraints (black color) and theoretical constraints denoted by red color which show the regions forbidden either due to lack of REWSB (lower right region) or because $\tilde{\tau}_1$ is the LSP (upper left region).

One can see that for both positive and negative μ the the highest value for σ_{SI} is about 10^{-6} pb. This happens in two regions: either in the lower left corner of the m_0 vs. $m_{1/2}$ parameter space where the exchanged squark masses are light, or in the HB/FP region for large m_0 values and low-intermediate $m_{1/2}$ values (gray and green colors), along the border of the red forbidden region where REWSB does not occur. In this region, there is a large higgsino component to the neutralino, which enhances the Z -exchange contribution to σ_{SI} . For $\mu > 0$, the lowest cross sections reach below 10^{-10} pb and occur at very large values of m_0 and $m_{1/2}$ where squark masses are high, thus suppressing the overall scattering cross section. For $\mu < 0$, the lowest cross section values can dip far below 10^{-12} pb in the magenta-shaded regions. The nature of this behavior in σ_{SI} is due to a cancellation between processes involving up - and $down$ -type quarks where the leading contribution comes from t -channel Higgs boson exchange [21].

In Fig. 2 we plot σ_{SI} versus neutralino mass for a random scan over mSUGRA parameter space for various $\tan \beta$ and $A_0 = 0$, for $\mu < 0$ (top frame) and $\mu > 0$ bottom frame). Parameter space points which satisfies only theoretical and LEP2 constraints (*i.e.* parameter space presented in Fig. 1) are represented by small dots. If instead we restrict $\Omega_{\tilde{Z}_1} h^2$ to be within the experimental limits $0.0945 < \Omega_{CDM} h^2 < 0.129$, only the solid circles survive. The different colors of the dots correspond to different values of $\tan \beta$. We can see now how restrictive the relic density constraint is for the parameter space and for the range of σ_{SI} . One can see that the maximum value σ_{SI} can be reduced almost by an order of magnitude for some values of $\tan \beta$. We also show in these plots the reach of Stage 1, Stage 2 and Stage 3 experiments. Evidently Stage 1 experiments are just now starting to explore regions of mSUGRA model parameter space. Stage 2 and Stage 3 detectors can explore much larger regions of parameter space, but none of the planned detectors will be able to completely rule out SUSY dark matter.

The regions of parameter space allowed by the relic density constraint form branches of distinct patterns. One sort of branch is the HB/FP region. It is exhibited by region of almost constant $\sigma_{SI} \sim 10^{-8}$ pb which is nearly independent of $\tan \beta$. In this region, it is possible to satisfy not only the relic density constraints, but also (as shown below) a_μ and $BF(b \rightarrow s\gamma)$ constraints. One can solve the SUSY flavor and CP problems, and possibly

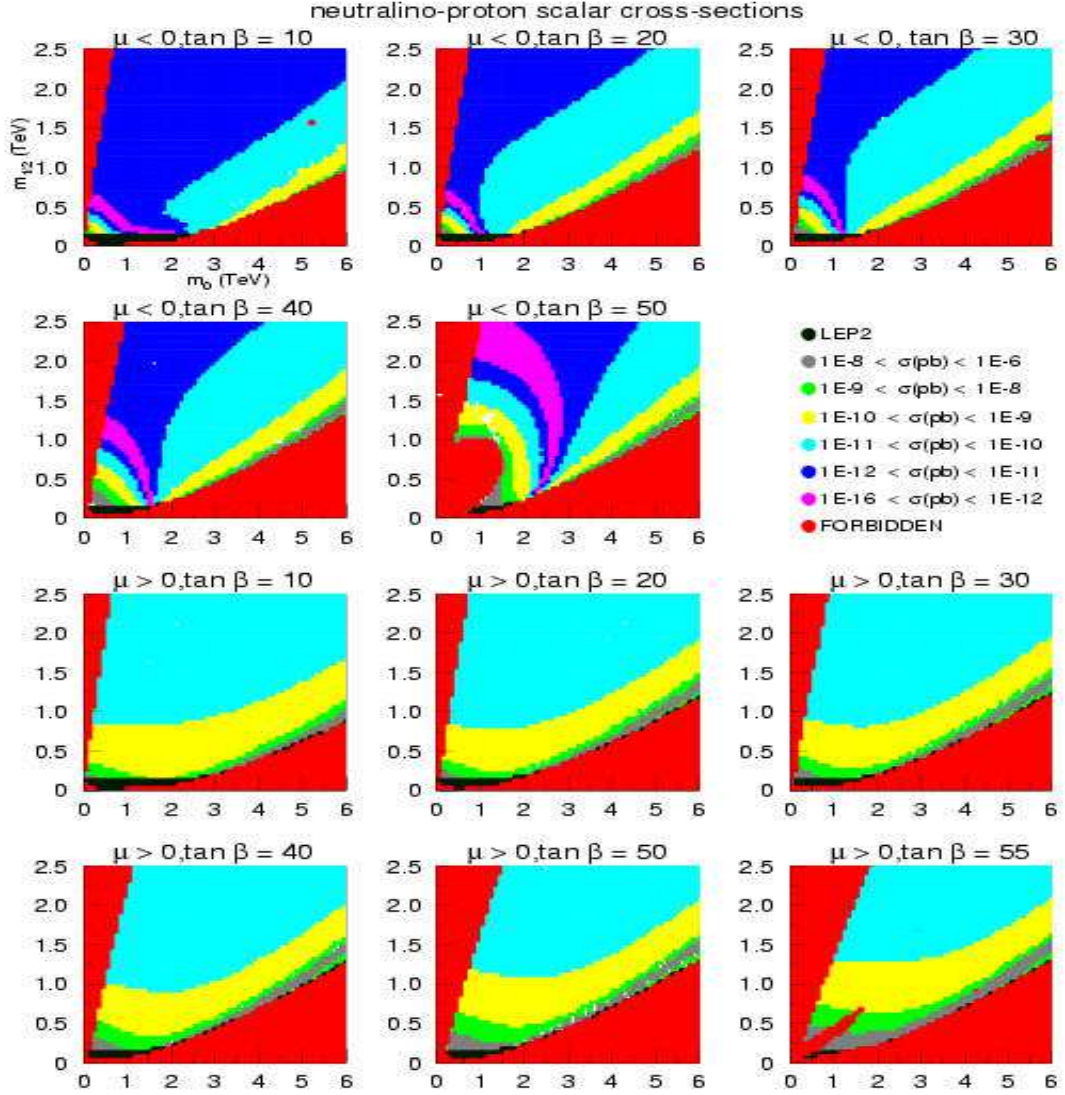


Figure 1: Cross section rates for spin-independent neutralino-proton scattering in the mSUGRA model for $A_0 = 0$.

maintain naturalness. The Stage 3 detectors ought to have sufficient reach to cover this interesting region of model parameter space!

In Fig. 3a.), we show σ_{SI} vs. $m_{\tilde{Z}_1}$ as a function of the complete model parameter space for $\mu < 0$. The ranges of parameters are listed above the figure, and include a scan over all A_0 values. We also show the reach of Stage 1, 2 and 3 detectors. Most points in mSUGRA model parameter space are now excluded by the WMAP constraint, so we show points with $0.094 < \Omega_{\tilde{Z}_1} h^2 < 0.129$ by green dots, while blue dots denote points with $\Omega_{\tilde{Z}_1} h^2 < 0.094$, which would require in addition some form of non-MSSM cold dark matter. The corresponding plot of σ_{SI} vs. $\Omega_{\tilde{Z}_1} h^2$ is shown in frame b.). The parameter space with

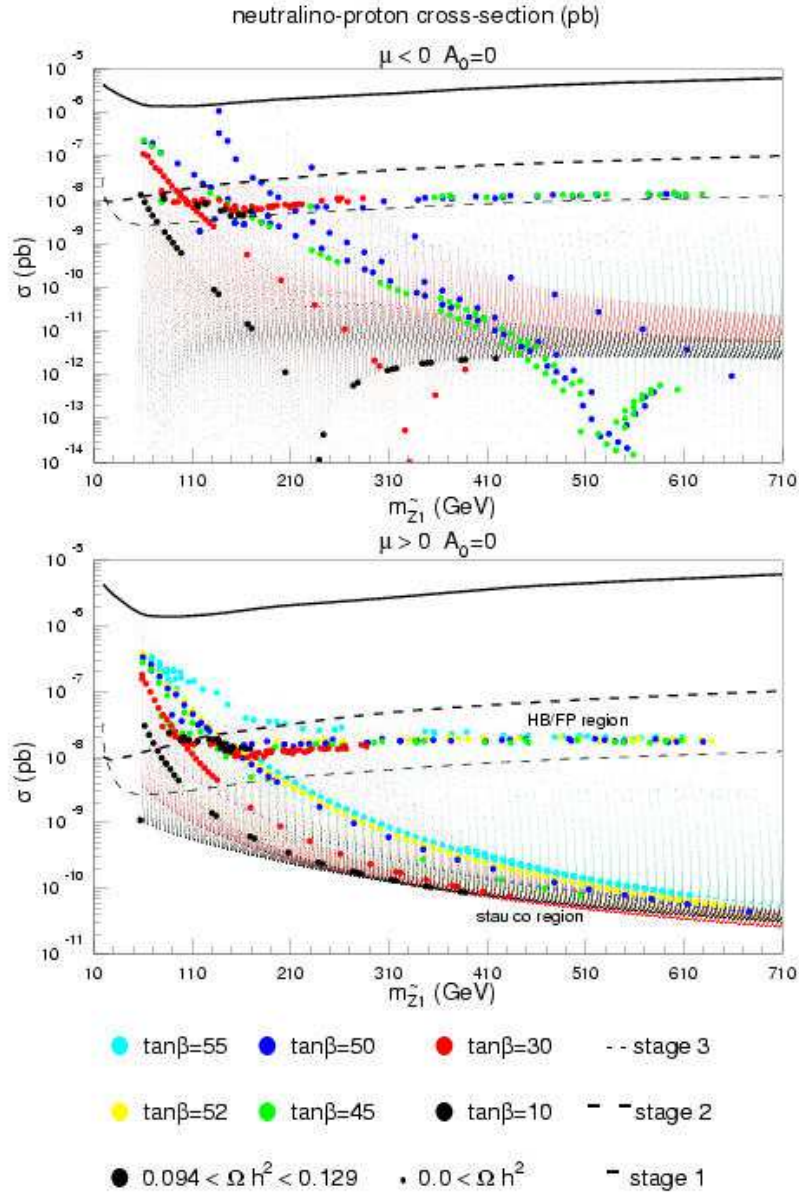


Figure 2: σ_{SI} versus neutralino mass

$\mu > 0$ is shown in frames *c.*) and *d.*). In the case of $\mu < 0$, much lower cross-sections are allowed, due to the above mentioned cancellations in quark-neutralino effective couplings. However, it is the $\mu < 0$ sign which is more restricted by a_μ and $BF(b \rightarrow s\gamma)$ constraints.

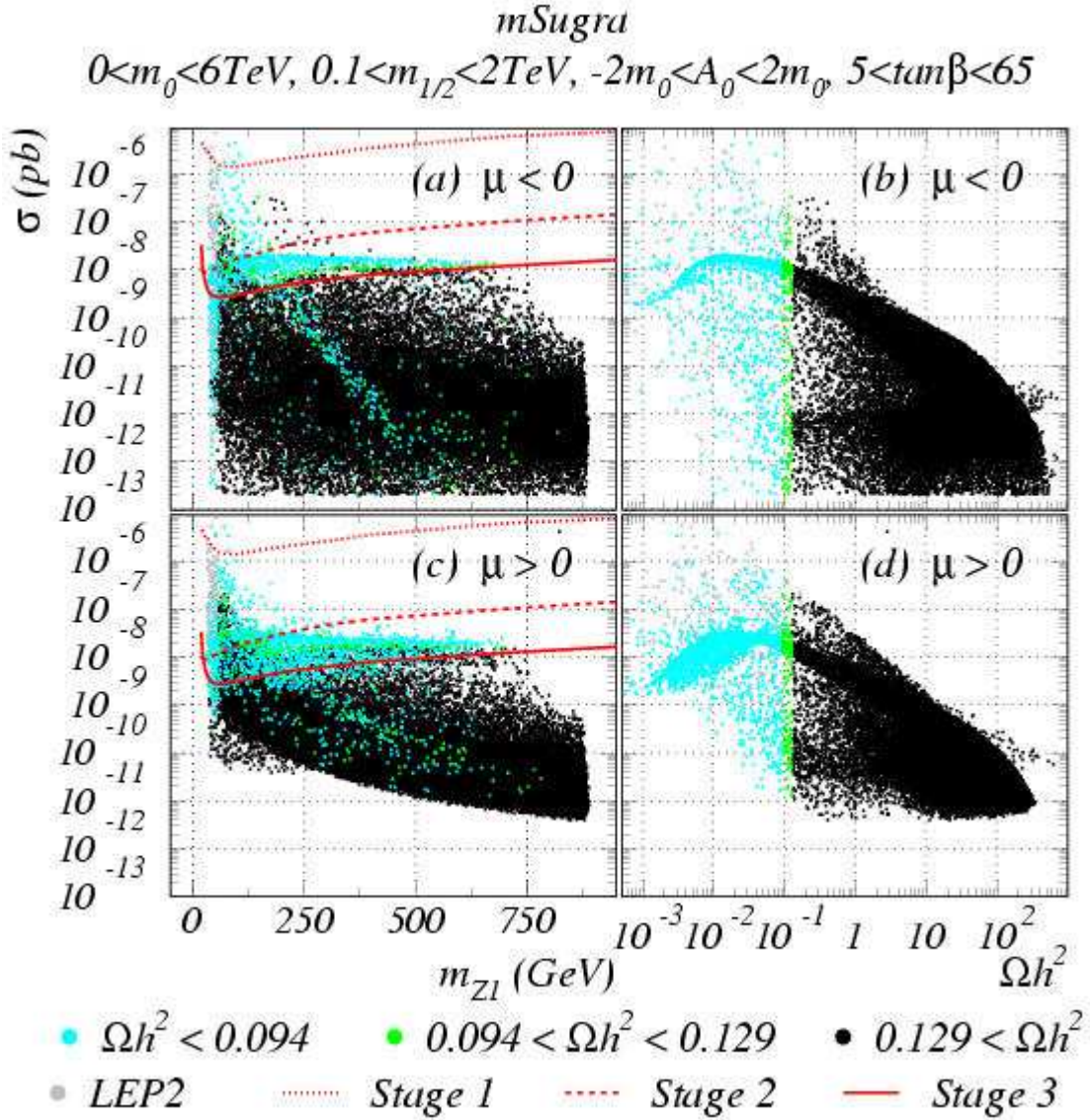


Figure 3: In a) we plot cross section rates *vs.* $m_{\tilde{Z}_1}$ for a scan over mSUGRA parameter space with $\mu < 0$. In b), we show cross section *vs.* $\Omega_{\tilde{Z}_1}^2 h^2$ for the same $\mu < 0$ parameter space. In c) and d), we show the same plots, except for $\mu > 0$.

Finally we present our results on σ_{SI} for mSUGRA together with the above mentioned direct and indirect constraints in Fig. 4 for the m_0 *vs.* $m_{1/2}$ plane. As an example we have chosen $\tan\beta = 10$, $\mu > 0$ (upper left), $\tan\beta = 30$, $\mu > 0$ (upper right), $\tan\beta = 45$, $\mu < 0$ (bottom left) and $\tan\beta = 55$, $\mu > 0$ (bottom right) cases for $A_0 = 0$. The red and black shaded regions are excluded due to lack of REWSB or a stau LSP respectively. The magenta region is excluded by LEP2 searches for charginos and sleptons. The region below the red curve is excluded by LEP2 Higgs searches. One can see how $BF(b \rightarrow s\gamma)$ (magenta contours), a_μ (blue contours), $B_s \rightarrow \mu^+\mu^-$ (light blue contours) can further significantly

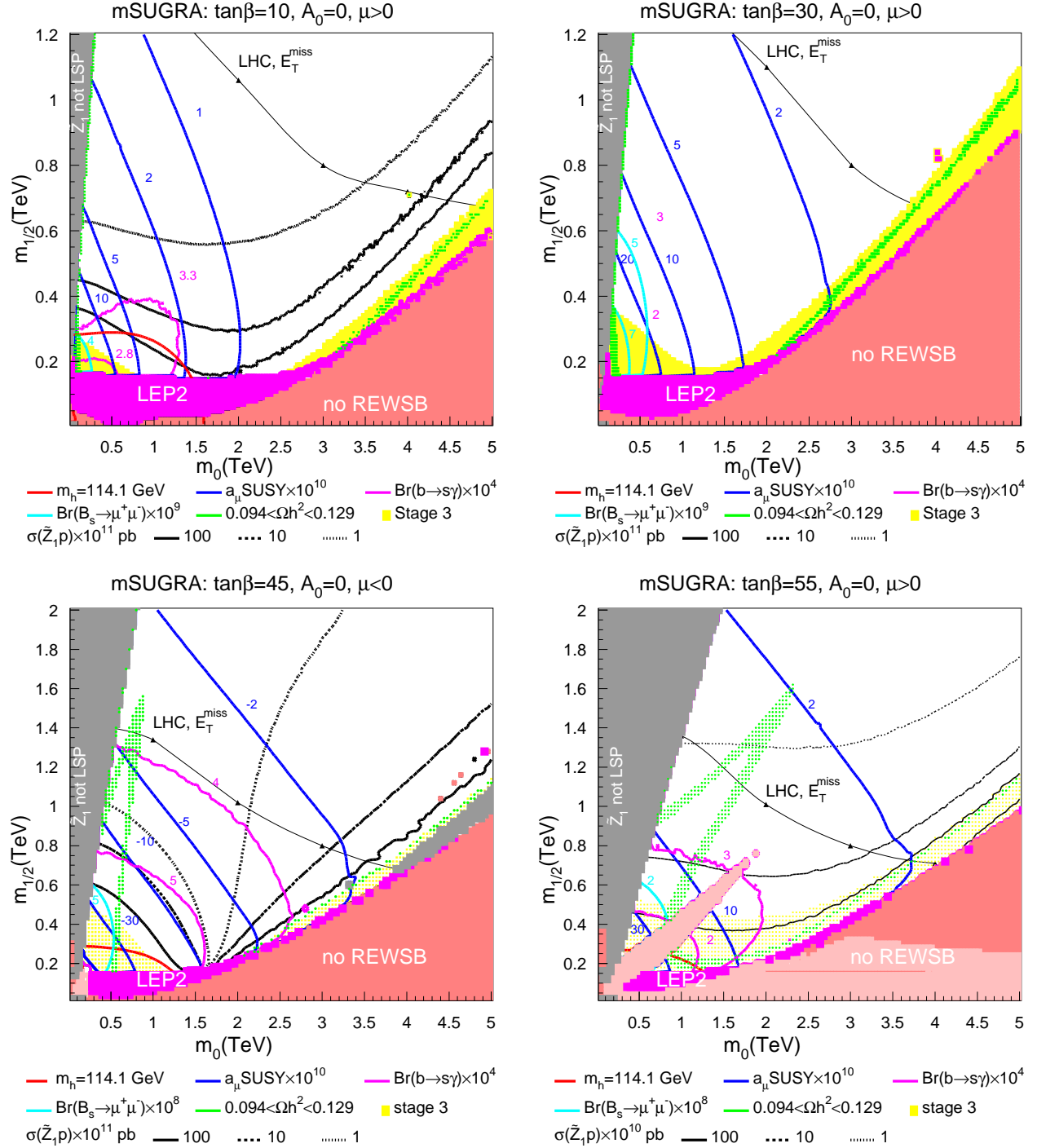


Figure 4: Constraints and σ_{SI} rates for mSUGRA model in m_0 vs. $m_{1/2}$ plane: $\tan\beta = 10, \mu > 0$ (upper left), $\tan\beta = 30, \mu > 0$ (upper right), $\tan\beta = 45, \mu < 0$ (bottom left) and $\tan\beta = 55, \mu > 0$ (bottom right), $A_0 = 0$.

reduce MSSM parameter space and the range of σ_{SI} .

For $\tan\beta = 10$, there are three regions of allowed relic density (which could be also

recognized by looking at different branches of Fig. 2):

- 1) lower left “bulk” region where neutralinos annihilate dominantly through t -channel slepton exchange;
- 2) the region of $\tilde{\tau}_1 - \tilde{Z}_1$ co-annihilation which is along the stau LSP region[54]. One should notice that this region has highly fine-tuned relic density since a small variation in m_0 would lead to a large change in Ωh^2 [55, 41];
- 3) HB/FP region where μ becomes small and a large higgsino component of \tilde{Z}_1 allows for efficient annihilation into WW , ZZ , Zh and hh pairs [56, 41].

In the first bulk region, σ_{SI} is the highest and reaches $10^{-6} - 10^{-7}$ pb level (Fig.2). It can be easily accessible by future experiments on direct CDM searches as indicated by yellow region in Fig. 4. Unfortunately it is already excluded by the LEP2 bound on m_h . It also has a rather low value of $BF(b \rightarrow s\gamma)$.

The narrow $\tilde{\tau}_1 - \tilde{Z}_1$ co-annihilation region lacks theoretical attraction due to large fine-tuning in the relic density, and it is also not attractive for direct DM search experiments. The typical level of σ_{SI} is $10^{-10} - 10^{-11}$ pb (dashed and dotted black contours for $\tan \beta = 30$ in Fig. 4), and in this region it will be not accessible even by Stage 3 detectors.

Finally, from both a theoretical and experimental point of view, the HB/FP region looks very attractive. One can see from Fig. 2 (dashed line) and Fig. 4 (yellow shaded region) that Stage 3 experiments on direct CDM search can indeed entirely cover this region.

If we increase $\tan \beta$ to 30, as shown in Fig. 4 upper-right, then most of the bulk region of relic density is still excluded by a combination of Higgs mass and $BF(b \rightarrow s\gamma)$ constraints. The stau co-annihilation region remains narrow and largely beyond reach of direct DM detection experiments, and the HB/FP region remains consistent with all constraints, along with having a large rate of direct DM detection. However, by increasing $\tan \beta$ to 45 ($\mu < 0$) (Fig. 4, bottom-left) and $\tan \beta = 55$ ($\mu > 0$) (Fig. 4, bottom-right) a qualitatively new region (fourth kind of region) of allowed relic density appears. One can see the diagonal strip running from the lower-left to the upper-right corner. In this region, neutralinos annihilate efficiently through the s -channel A and H bosons which have very large widths due to large b - and τ -Yukawa couplings. Though these regions are also theoretically attractive, one can see that they will be inaccessible by neutralino direct search experiments.

Finally, we would like to stress the high degree of complementarity between the LHC SUSY search and the direct DM search in restricting supersymmetric parameter space. A very intriguing feature of the direct DM search experiments is that they can cover the entire HB/FP region while LHC can explore $m_{1/2}$ only up to about 700 GeV (largely independent of $\tan \beta$) [57]. On the other hand, LHC is able to completely cover the region of neutralino annihilation through heavy Higgs resonances and almost all of the stau co-annihilation region [57]. Thus, a combination of the LHC and Stage 3 direct DM experiments together can cover almost the entire mSUGRA parameter space!

4. Results for Yukawa unified models

In this Section we present results for MSSM models with non-universal boundary conditions motivated by $SO(10)$ SUSY GUT scenarios. SUSY GUTs based on $SO(10)$ are theoretically very attractive. Along with gauge coupling unification, they unify all matter of a single generation into a single 16 dimensional spinorial multiplet of $SO(10)$. The 16 dimensional spinorial multiplet contains a right-handed neutrino which becomes a SM gauge singlet. It can be used to provide for massive neutrinos via the see-saw mechanism. The massive neutrino states may play an important role in baryogenesis via intermediate scale leptogenesis [58] due to the structure of the neutrino sector. Finally, $SO(10)$ is an anomaly-free group and explains the cancellation of triangle anomalies within the SM.

In the simplest models of $SO(10)$ SUSY GUTs, the two MSSM Higgs doublets are both present in a single 10-dimensional representation. This structure of the Higgs sector leads to a crucial feature of the model — it predicts Yukawa coupling unification since the superpotential contains the term: $\hat{f} \ni f \hat{\psi}(\mathbf{16})^T \hat{\psi}(\mathbf{16}) \hat{\phi}(\mathbf{10}) + \dots$. In Ref. [30], we have searched model parameter space for solutions with a high degree of third generation Yukawa coupling unification, for both positive and negative values of the superpotential μ parameter. In the case of $\mu < 0$, there exist regions of SUSY parameter space satisfying all experimental constraints and possessing perfect Yukawa coupling unification. Yukawa unified solutions for $\mu > 0$ were also found. These latter solutions required multi-TeV values of the GUT scale scalar mass parameter m_{16} , and were in general difficult to reconcile with bounds on the relic density of neutralinos.

We have adopted results from [30] using Isajet v7.64 and studied the neutralino-proton scattering cross section for cases with a high degree of Yukawa coupling unification. The measure of Yukawa unification used is given by

$$R = \max(f_t, f_b, f_\tau) / \min(f_t, f_b, f_\tau), \quad (4.1)$$

where f_t , f_b and f_τ are the t , b and τ Yukawa couplings, and R is measured at $Q = M_{GUT}$. In $SO(10)$ models, the reduction in rank of the gauge symmetry group can lead to additional D -term contributions to scalar particle masses. In the case of $SO(10) \rightarrow SU(5) \times U(1)_X \rightarrow SU(3)_c \times SU(2)_L \times U(1)_Y$, the D -term contributions lead to the following GUT scale scalar mass splittings (DT model):

$$\begin{aligned} m_Q^2 &= m_E^2 = m_U^2 = m_{16}^2 + M_D^2, \\ m_D^2 &= m_L^2 = m_{16}^2 - 3M_D^2, \\ m_N^2 &= m_{16}^2 + 5M_D^2, \\ m_{H_{u,d}}^2 &= m_{10}^2 \mp 2M_D^2, \end{aligned}$$

where M_D^2 parameterizes the magnitude of the D -terms. Owing to our ignorance of the gauge symmetry breaking mechanism, M_D^2 can be taken as a free parameter, with either positive or negative values. $|M_D|$ is expected to be of order the weak scale. An alternative scenario is for mass splittings to occur only for GUT scale scalar Higgs masses[59] (HS

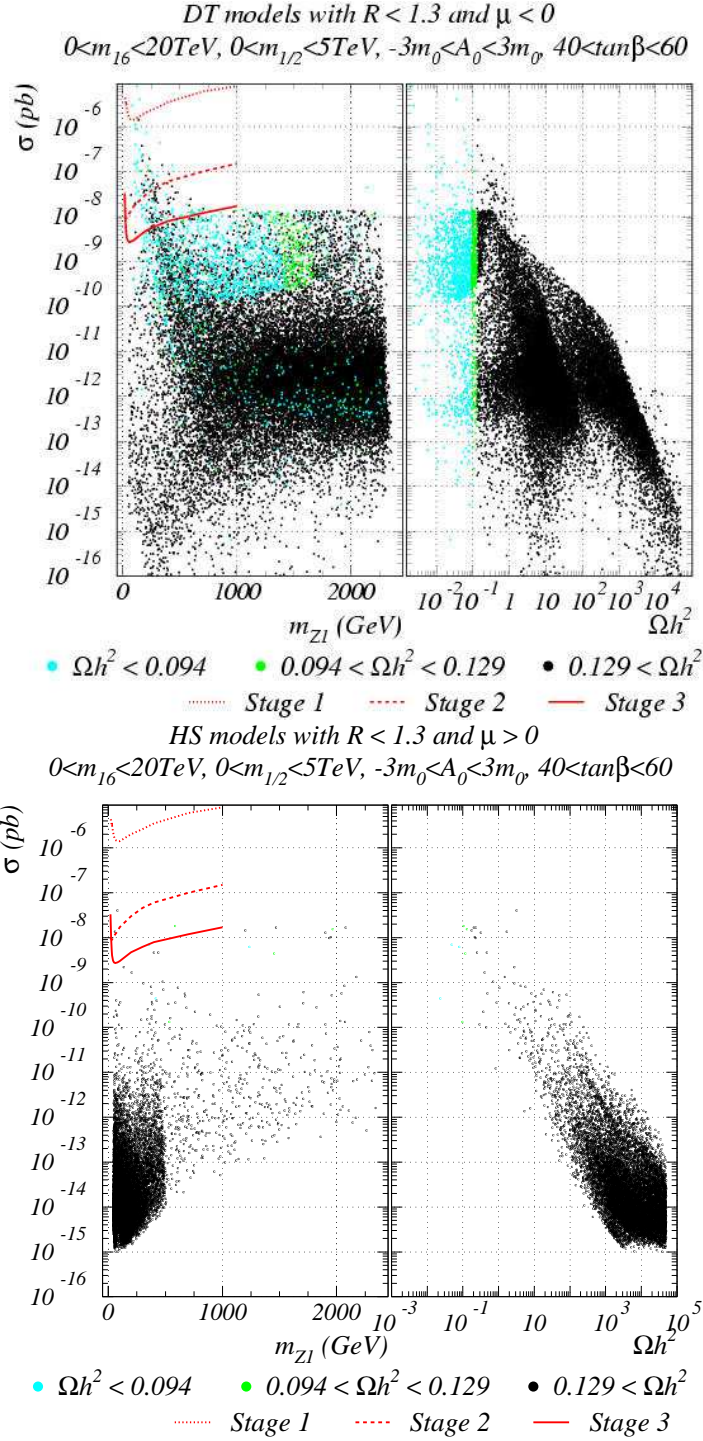


Figure 5: Scattering spin-independent neutralino-proton rates versus neutralino mass(left) and Ωh^2 (right) for *DT*(top) and *HS*(bottom) models

model) *i.e.*

$$m_Q^2 = m_E^2 = m_U^2 = m_{16}^2,$$

$$\begin{aligned}
m_D^2 &= m_L^2 = m_{16}^2, \\
m_N^2 &= m_{16}^2, \\
m_{H_{u,d}}^2 &= m_{10}^2 \mp 2M_D^2.
\end{aligned}$$

The *DT* model is slightly preferred for models with $\mu < 0$, while the *HS* model is preferred for $\mu > 0$. Both the *DT* and *HS* models are characterized by the following free parameters,

$$m_{16}, m_{10}, M_D^2, m_{1/2}, A_0, \tan \beta, \text{sign}(\mu).$$

We scan these models over the following parameter range:

$$\begin{aligned}
0 &< m_{16} < 20 \text{ TeV}, \\
0 &< m_{10} < 30 \text{ TeV}, \\
0 &< m_{1/2} < 5 \text{ TeV}, \\
-(m_{10}/\sqrt{2})^2 &< M_D^2 < +(m_{10}/\sqrt{2})^2, \\
40 &< \tan \beta < 60, \\
-3m_{16} &< A_0 < 3m_{16}.
\end{aligned} \tag{4.2}$$

Our results for Yukawa unified models are presented in Fig. 5 for $\mu < 0$ *DT* model (upper frames) and for $\mu > 0$ *HS* model (lower frames). In each, we require $R < 1.3$. The left-most frames show σ_{SI} vs. $m_{\tilde{Z}_1}$, while the right-most frames show σ_{SI} vs. $\Omega_{\tilde{Z}_1} h^2$. Green points fall within the WMAP limits on the relic density, while blue points have $\Omega_{\tilde{Z}_1} h^2 < 0.094$. Black points have $\Omega_{\tilde{Z}_1} h^2 > 0.129$. We see immediately from the relatively infrequent number of green points how restrictive the WMAP bounds are on Yukawa unified models. Nevertheless, some Yukawa unified models are consistent with WMAP. These models tend to have relatively heavy sparticle mass spectra, and usually fulfill the $\Omega_{\tilde{Z}_1} h^2$ bound by having $2m_{\tilde{Z}_1} \sim m_A$ so that resonance neutralino annihilation via heavy and pseudoscalar Higgs bosons occurs at a high rate[30]. The WMAP allowed models tend to have direct detection rates below the reach of even the Stage 3 DM search experiments. We do note, however, that several points do occur with allowed relic densities that are accessible to direct DM searches.

In the lower two frames, we show the corresponding results for *HS* models with $\mu > 0$. In this case, m_{16} values of 8 – 20 TeV are favored. The SUSY particle spectra is characterized by an inverted scalar mass hierarchy, so that the models may still satisfy naturalness criteria, since third generation scalar can be relatively light. However, the very heavy spectra leads usually to too high of values of $\Omega_{\tilde{Z}_1} h^2$, and also suppresses the direct detection rate to below the reach of even Stage 3 detectors. Again we note that a few points do survive the relic density constraint, and one is even within reach of Stage 3 experiments.

It is also useful to examine the Yukawa unified models in the context of constraints from $BF(b \rightarrow s\gamma)$, a_μ and $BF(B_s \rightarrow \mu^+\mu^-)$. We illustrate this in Fig. 6, where we present contours of the σ_{SI} together with experimental constraints in the m_{16} vs. $m_{1/2}$ plane. The left frame of Fig. 6 presents results for $\mu < 0$ and $m_{10} = 1.356m_{16}$, $M_D = 0.394m_{16}$, $A_0 = 0$

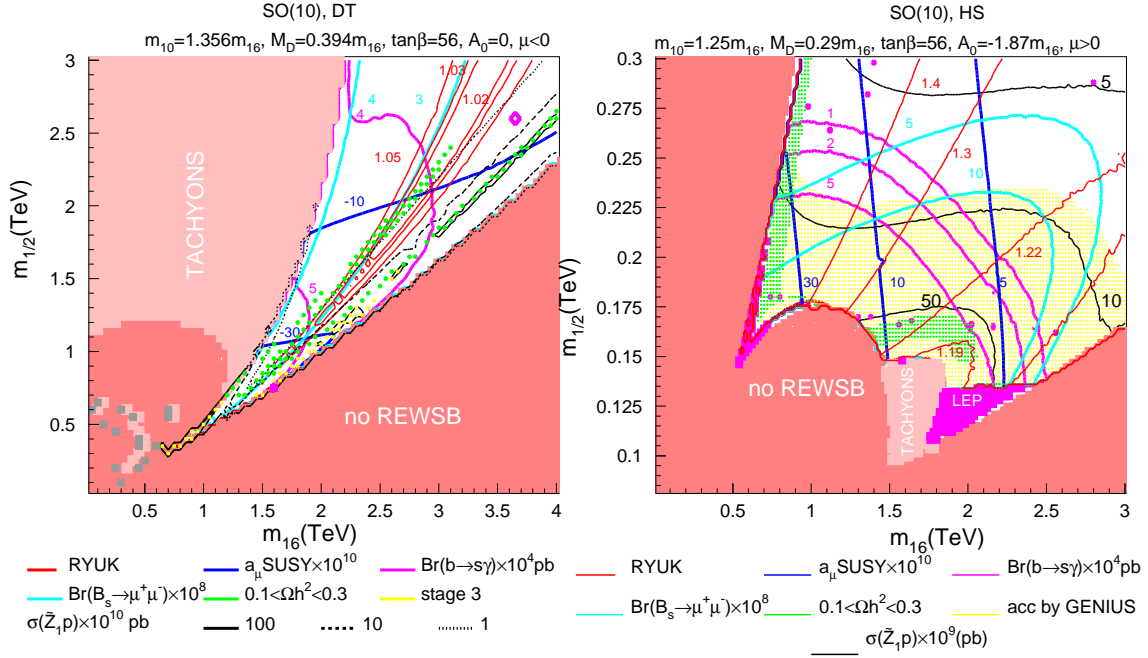


Figure 6: Constraints and σ_{SI} rates in m_0 vs. $m_{1/2}$ plane for *DT*(left) and *HS*(right) models

and $\tan\beta = 56$, which leads to a central region of the plot with good Yukawa unification (illustrated by the $R < 1.02 - 1.05$ contours). One can see that the region of good Yukawa coupling unification can satisfy all experimental constraints with a small $b \rightarrow s\gamma$ pull. The valid region is marginal for the future direct CDM search experiments which is indicated by the yellow region. The value of σ_{SI} can be quite high $\sim 10^{-7}$ pb in the lower left corner but $BF(b \rightarrow s\gamma)$ is too high in this region (magenta contour) and therefore it is excluded. In addition this corner of parameter space is excluded by experimental constraint on a_μ since its deviation from the SM is below $a_\mu = -30 \times 10^{-10}$ (blue contour) level. There is also a HB/FP region near the right hand excluded region where the relic density falls within the $0.1 - 0.3$ level, and neutralinos may be directly detected. This region is somewhat removed from the central area where Yukawa unification is best.

We illustrate results for the *HS* model with $\mu > 0$ in the right most frame, where the parameter set was chosen to give reasonable values of the neutralino relic density and to have Yukawa unification at the order of 20%. The left most side has a good relic density value but poor Yukawa unification. The low $m_{1/2}$ region has an area of good relic density (due to neutralino annihilation through the light Higgs h pole) and Yukawa coupling unification below $R = 1.19$. While much of this region is accessible to direct DM searches, much of it is also gives values of $BF(b \rightarrow s\gamma)$ outside of the window of expectation.

5. Gaugino mediated SUSY breaking models with non-universal gaugino masses

As mentioned in the introduction, the formulation of SUSY GUTs in extra dimensions yields elegant solutions to many of the problems encountered by four-dimensional models[34]. Recently, SUSY GUT models have been formulated in five and even higher dimensions[33]. Models have been constructed wherein the doublet-triplet splitting problem is simply solved, and where proton decay is either suppressed or forbidden. R -parity conservation may also naturally arise. All these facets may arise without the need for the large Higgs representations which are needed to break the GUT symmetry in 4-d models.

In 5-d models, compactification of the extra dimension on an $S^1/(Z_2 \times Z'_2)$ orbifold leads to two inequivalent fixed points identified as separated 4-dimensional branes within the 5-d bulk. Only fields with positive parities under the Z_2 and Z'_2 symmetries have massless Kaluza-Klein modes. The Z_2 parity assignments are chosen so that the $N = 1$ SUSY in 5-d, which normally reduces to $N = 2$ SUSY in 4-d, in fact breaks to $N = 1$ SUSY in 4-d. Superfields containing MSSM matter are assumed to exist on the observable brane, while the “hidden” brane is set up to accomodate SUSY breaking. The Z'_2 parity assignments are made so that the grand unified symmetry is broken on the hidden brane. The set up is well suited to accomodate SUSY breaking via gaugino mediation, wherein SUSY breaking is communicated from the hidden brane to the visible brane via gauge superfields which propagate in the bulk[60]. In gaugino mediated SUSY breaking (inoMSB), the scalar, trilinear and bilinear soft SUSY breaking masses are loop suppressed, and can effectively be taken to be zero. The gaugino masses however are non-zero.

Several intriguing scenarios arise in gaugino mediation. In all cases, in the 4-d effective theory below $\min(M_c, M_{GUT})$, $m_0 \sim A_0 \sim 0$, while non-zero μ and B can be generated. These latter parameters are traded for $\tan \beta$ and M_Z , as is usual where electroweak symmetry is broken radiatively. The scenarios are given as follows.

- 1. If $SU(5)$ is the gauge symmetry on the hidden brane, then universal gaugino masses will result. In this case, gaugino mediation leads to a stau LSP unless additional above-the-GUT-scale RGE running is allowed (Schmaltz-Skiba case)[61, 62].
- 2. If $SU(5)$ is the gauge symmetry of the bulk, but is broken to the SM gauge symmetry on the hidden brane, then independent gaugino masses are induced. The effective 4-d theory on the visible brane is just the MSSM, with parameter space $M_1(M_c)$, $M_2(M_c)$, $M_3(M_c)$, $\tan \beta$ and $sign(\mu)$.
- 3. If $SO(10)$ is the bulk symmetry, and is broken to $SO(6) \times SO(4)$ (isomorphic to the Pati-Salam group $SU(4) \times SU(2)_L \times SU(2)_R$) on the hidden brane, and $SO(10)$ is broken to $SU(5)$ on the visible brane via the usual Higgs mechanism, then the visible sector model obeys parameter space is given by $M_2(M_c)$, $M_3(M_c)$, $\tan \beta$ and $sign(\mu)$, where $M_1 = \frac{2}{5}M_3 + \frac{3}{5}M_2$ at $Q = M_c$ (Dermisek-Mafi case)[31, 63].

- 4. If $SO(10)$ is the bulk gauge symmetry, and flipped $SU(5)' \times U(1)'$ is the hidden brane symmetry, then the parameter space is given by $M_1(M_c)$, $M_2(M_c)$, $\tan\beta$ and $sign(\mu)$, where $M_3(M_c) = M_2(M_c)$ (Barr-Dorsner case)[64].

In this section, we explore the direct dark matter detection rates for the latter three cases of non-universal gaugino mediation. In these models, the additional parameter freedom arising from non-universal gaugino mediation can be exploited to solve the slepton LSP problem, instead of above-the-GUT scale running suggested by Schmaltz and Skiba. Hence, in our calculations, we adopt the choice of $M_c = 1 \times 10^{16}$ GeV, *i.e.* near but just below the usual unification scale of $M_{GUT} \simeq 2 \times 10^{16}$ GeV. This choice preserves the prediction of gauge coupling unification.

Our main results are shown in Fig. 7 for case 2 with independent gaugino masses at the compactification scale. We have scanned over the parameter space limits as listed at the top of the figure. Solutions which yield a spectrum with a neutralino LSP are listed by dots. These solutions usually have a lightest neutralino with a substantial wino or higgsino component, since $M_1(M_c)$ must be chosen to be large enough to contribute to RG running of $m_{\tilde{T}R}^2$ so that it avoids becoming the LSP. Neutralinos with a large wino or higgsino component can annihilate at high rates to WW , ZZ and Zh pairs so that they generally give a rather low value of the relic density[65]. Thus, supersymmetric dark matter would have to be augmented by other forms of dark matter to match the constraints on $\Omega_{CDM}h^2$ from WMAP and other measurements. Solutions with $\Omega_{\tilde{Z}_1}h^2 > 0.129$ are given by black dots, and would be excluded. Green dots denote solutions with $0.094 < \Omega_{\tilde{Z}_1}h^2 < 0.129$, and would not require other sources of dark matter. Finally, the light and dark blue dots have $\Omega_{\tilde{Z}_1}h^2 < 0.094$. The light blue solutions correspond to those with high $\tan\beta > 40$, while light blue solutions have $5 < \tan\beta < 40$.

We see from the plot that a significant number of solutions are accessible to Stage 1, Stage 2 and Stage 3 detectors. However, almost all these solutions have very low values of relic density. The experimental projections has been done under assumption that the *local* CDM density measured from the galactic rotation curves is $\simeq 0.3$ GeV/cm³. If we assume that the local neutralino relic density contribution is just some fraction of the total local CDM density, then one needs to rescale experimental projections with a factor equal to this fraction.

While the scans over the complete parameter space are comprehensive, it can be instructive to plot results in particular parameter space planes. We present a scan of the M_2 vs. M_3 parameter space in Fig. 8 for $\mu > 0$ and $\tan\beta = 10$ with $M_1 = 1$ TeV (left frame) and $\tan\beta = 40$, $M_1 = 1.5$ TeV (right frame). It is easy to see that taking M_2 or M_3 too large will result in a model with a non-neutralino LSP, while taking M_3 too small results in a breakdown in REWSB. Taking M_2 too small results in a chargino mass in violation of LEP2 limits. The green regions give viable solutions which have in addition $\Omega_{\tilde{Z}_1}h^2 < 0.129$. The yellow-green regions in addition should be accessible to Stage 3 direct DM detection experiments. We also show various contours of m_h values, $b \rightarrow s\gamma$ branching fraction and a_μ . Whether or not any of these additional constraints are invoked, it is clear that much of the parameter space would be accessible to direct detection searches,

Independent gaugino masses with $M_{H_{u,d}}(M_c) = 0$
 $-10 < M_1 < 10 \text{ TeV}$, $-3 < M_2 < 3 \text{ TeV}$, $-2 < M_3 < 2 \text{ TeV}$, $5(40) < \tan\beta < 60$
 $2.16 < \text{BF}(b \rightarrow s\gamma) \times 10^4 < 4.34$, $-16.7 < a_\mu^{\text{SUSY}} \times 10^{10} < 49.1$

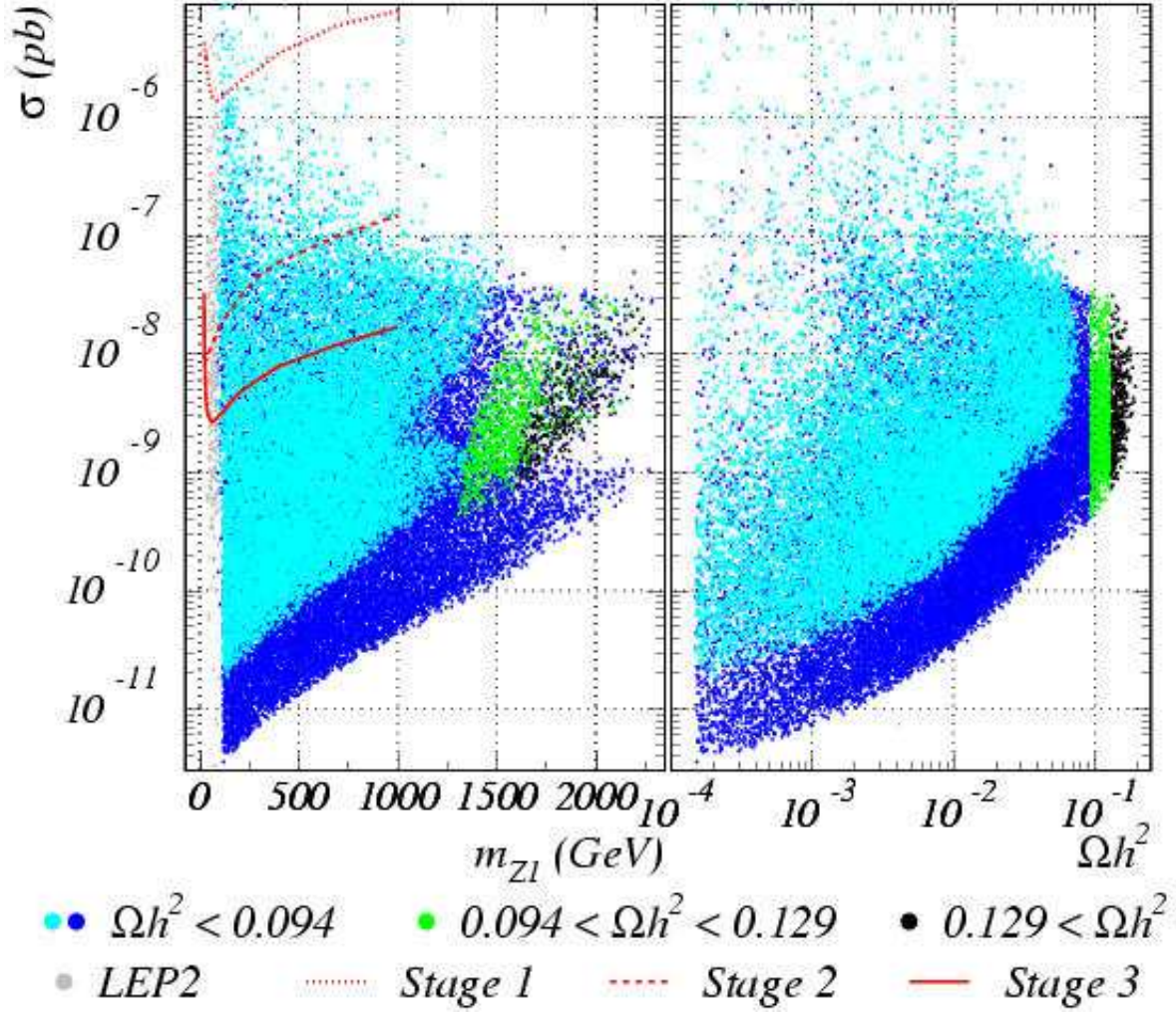


Figure 7: Constraints and σ_{SI} rates for independent gaugino mass scenario.

assuming that neutralino dark matter makes up the bulk of the local relic density.

If case 3 with $SO(10)$ breaking to the Pati-Salam group is invoked, then the parameter space becomes more restrictive, since now M_1 is determined by the choice of M_2 and M_3 . In this case, we again plot parameter space in Fig. 9 in the M_2 vs. M_3 plane for $\tan\beta = 5$ (left) and 10 (right), with $\mu > 0$. The viable parameter space is again denoted by the green color, with experimental constraints indicated by various contours. Much higher values of $\tan\beta$ result in almost no viable parameter space[63]. The yellow-green regions again denote parameter space accessible to Stage 3 experiments.

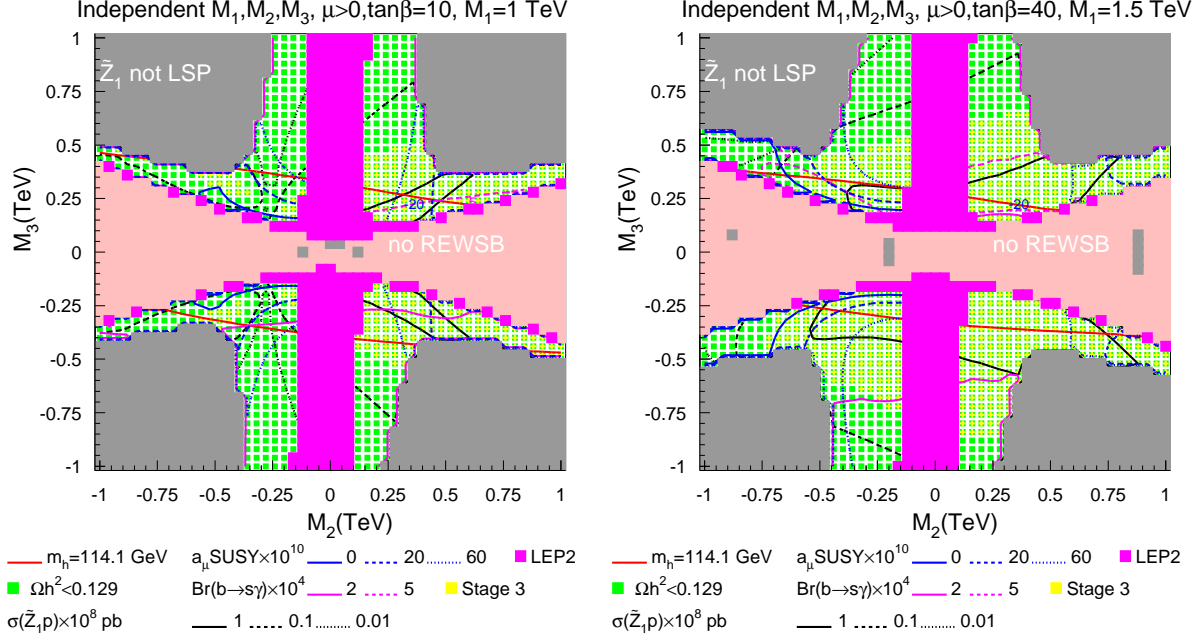


Figure 8: Constraints and σ_{SI} rates for independent gaugino mass scenario in $(M_2 - M_3)$ plane

The M_2 vs. M_1 parameter space with $M_2 = M_3$ for the case of $SO(10)$ breaking to flipped $SU(5)$ is presented in Fig. 10, for $\tan\beta = 10$ (left) and 40 (right), and for $\mu > 0$. One can see that the parameter space opens up with increasing M_1 , and moreover, that the relic density is safely below the WMAP upper limit. The region with very low values of M_2 is excluded because the chargino mass falls below limits from LEP2. For higher (but still low) values of M_2 , the lightest neutralino is dominantly wino-like, and has a large scattering cross section with protons, and may be accessible to Stage 3 direct detection searches.

6. Conclusions

In this paper, we have evaluated the neutralino-proton scattering cross section in 1.) the mSUGRA model, 2.) in $SO(10)$ SUSY GUT models with Yukawa coupling unification, and 3.) in extra-dimensional SUSY GUT models with gaugino-mediated SUSY breaking and non-universal gaugino masses. Our results for the mSUGRA model give a comprehensive scan of σ_{SI} over model parameter space using Isajet v7.65. We also compared the DM detection rate against other constraints including those on the neutralino relic density from recent WMAP data, the $b \rightarrow s\gamma$ branching fraction and the muon anomalous magnetic moment a_μ . The relic density constraint yields only several viable regions of parameter space: the bulk region at low m_0 and $m_{1/2}$, the stau co-annihilation region at low m_0 , the HB/FP region at large m_0 , and the Higgs resonance annihilation region at large $\tan\beta$. The bulk region contains relatively light slepton masses of 300-600 GeV, so that neutralinos

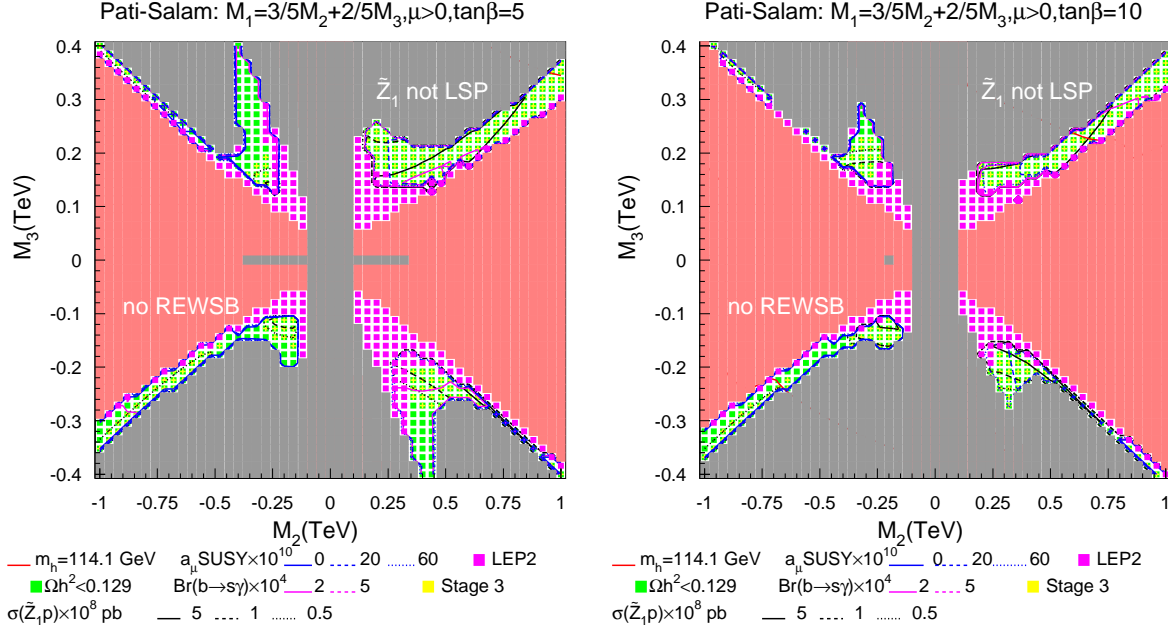


Figure 9: Constraints and σ_{SI} rates for Pati-Salam scenario in $(M_2 - M_3)$ plane

can annihilate via t -channel graphs in the early universe. The relatively light sparticle mass spectra associated with this region yields observable rates for direct detection of dark matter, but can also lead to values of m_h , $BF(b \rightarrow s\gamma)$ and/or a_μ in violation with experimental limits. The stau co-annihilation region and Higgs resonance region typically have heavy sparticle mass spectra, and low direct detection rates, while the HB/FP region has low $|\mu|$ values and neutralinos with a significant higgsino component. This latter quality allows for large neutralino annihilation cross sections in the early universe, and also for observable rates for direct DM detection. Evidently direct DM search experiments can probe the entire viable HB/FP region. This is fortuitous, since this region is difficult to access via the CERN LHC or a linear e^+e^- collider. Meanwhile, the CERN LHC can probe essentially all the Higgs annihilation region at large $\tan\beta$, and almost all of the stau co-annihilation region. Our analysis illustrates the complementarity of collider searches for supersymmetric matter with direct searches for relic DM particles.

We also examined two classes of SUSY GUT models. The first, Yukawa unified $SO(10)$ models, have non-universal scalar masses. The constraint of Yukawa coupling unification along with indirect constraints from relic density, $b \rightarrow s\gamma$ and a_μ point to rather heavy SUSY spectra in these models. For $\mu < 0$, the relic density constraint can be accommodated by living in the Higgs annihilation corridor. But then sparticles must be rather heavy, and direct detection rates are usually, but not always, low. For $\mu > 0$, multi-TeV scalar masses are required, and the model is characterized by a radiatively induced inverted mass hierarchy. The very heavy scalars suppress neutralino annihilation cross sections, so the

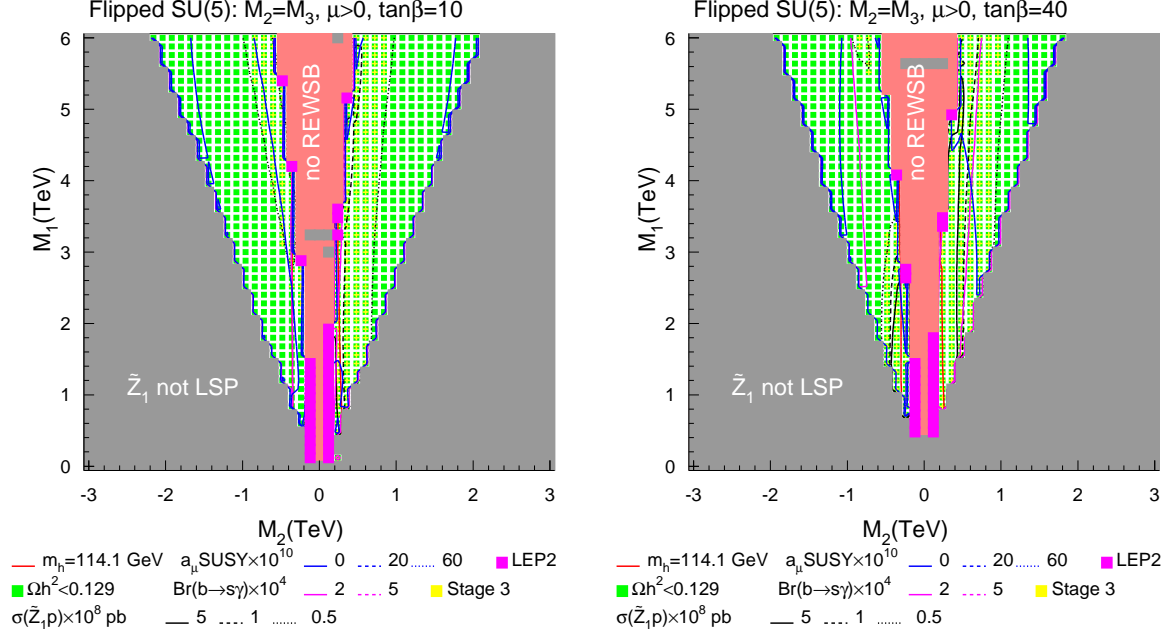


Figure 10: Constraints and σ_{SI} rates for flipped $SU(5)$ model in $(M_2 - M_3)$ plane

relic density is typically very large, and direct detection rates are very low.

The other class of models, extra dimensional SUSY GUTs with non-universal gaugino masses, require $m_0 \sim A_0 \sim 0$. But then the compactification scale gaugino mass M_1 must be typically larger than M_2 and M_3 to avoid a charged LSP. In this case, the LSP can be a neutralino, but with a significant wino or higgsino component (in mSUGRA, the LSP is almost always bino-like). This leads to large neutralino annihilation rates and a low relic density, but it also leads to large direct detection rates. However, experimental reach plots may have to be re-scaled according to assumptions regarding how much of the *local* relic density is composed of neutralinos, and not other forms of dark matter needed to match the WMAP constraints.

Acknowledgments

JO would like to thank V. Hagopian and H. Prosper for encouraging his work on this topic. This research was supported in part by the U.S. Department of Energy under contract number DE-FG02-97ER41022.

References

- [1] D. N. Spergel *et al.*, arXiv:astro-ph/0302209; C. L. Bennett *et al.*, arXiv:astro-ph/0302207.
- [2] For recent reviews, see *e.g.* S. Martin, in *Perspectives on Supersymmetry*, edited by G. Kane (World Scientific), hep-ph/9709356; M. Drees, hep-ph/9611409; J. Bagger,

- hep-ph/9604232; X. Tata, *Proc. IX J. Swieca Summer School*, J. Barata, A. Malbousson and S. Novaes, Eds., hep-ph/9706307; S. Dawson, Proc. TASI 97, J. Bagger, Ed., hep-ph/9712464.
- [3] For recent reviews see, *e.g.* A. Morales, Nucl. Phys. Proc. Suppl. **110**, 39 (2002) [arXiv:astro-ph/0112550]; Y. Ramachers, arXiv:astro-ph/0211500.
 - [4] H. Morales *et al.* (IGEX Collaboration), *Phys. Lett. B* **489** (2000) 268.
 - [5] H. V. Klapdor-Kleingrothaus, A. Dietz, G. Heusser, I. V. Krivosheina, D. Mazza, H. Strecker and C. Tomei, *Astropart. Phys.* **18**, 525 (2003) [arXiv:hep-ph/0206151].
 - [6] D. Abrams *et al.* [CDMS Collaboration], *Phys. Rev. D* **66**, 122003 (2002) [arXiv:astro-ph/0203500].
 - [7] A. Benoit *et al.*, *Phys. Lett. B* **545**, 43 (2002) [arXiv:astro-ph/0206271].
 - [8] H. V. Klapdor-Kleingrothaus, Nucl. Phys. Proc. Suppl. **110**, 364 (2002) [arXiv:hep-ph/0206249].
 - [9] R. Bernabei *et al.*, arXiv:astro-ph/0205047.
 - [10] N. Spooner, in *Proc. of the APS/DPF/DPB Summer Study on the Future of Particle Physics (Snowmass 2001)* ed. N. Graf, eConf **C010630**, E601 (2001).
 - [11] D. Cline *et al.*, *Prepared for 3rd International Conference on Dark Matter in Astro and Particle Physics (Dark 2000), Heidelberg, Germany, 10-16 Jul 2000*
 - [12] J. Dawson *et al.*, Nucl. Phys. Proc. Suppl. **110**, 109 (2002).
 - [13] D. B. Cline, H. g. Wang and Y. Seo, in *Proc. of the APS/DPF/DPB Summer Study on the Future of Particle Physics (Snowmass 2001)* ed. N. Graf, eConf **C010630**, E108 (2001) [arXiv:astro-ph/0108147].
 - [14] N. Spooner, in *Proc. of the APS/DPF/DPB Summer Study on the Future of Particle Physics (Snowmass 2001)* ed. N. Graf, eConf **C010630**, P401 (2001).
 - [15] J. I. Collar, J. Puibasset, T. A. Girard, D. Limagne, H. S. Miley and G. Waysand, *New J. Phys.* **2**, 14 (2000) [arXiv:astro-ph/0005059].
 - [16] N. Boukhira *et al.*, Nucl. Phys. Proc. Suppl. **110**, 103 (2002).
 - [17] M. W. Goodman and E. Witten, *Phys. Rev. D* **31**, 3059 (1985).
 - [18] K. Griest, *Phys. Rev. Lett.* **61**, 666 (1988); K. Griest, *Phys. Rev. D* **38**, 2357 (1988) [Erratum-*ibid.* **D 39**, 3802 (1989)];
 - [19] M. Drees and M. Nojiri, *Phys. Rev. D* **47**, 4226 (1993) and *Phys. Rev. D* **48**, 3483 (1993) [arXiv:hep-ph/9307208];
 - [20] H. Baer and M. Brhlik, *Phys. Rev. D* **57**, 567 (1998) [arXiv:hep-ph/9706509].
 - [21] J. R. Ellis, A. Ferstl and K. A. Olive, *Phys. Lett. B* **481**, 304 (2000) [arXiv:hep-ph/0001005];
 - [22] R. Barbieri, M. Frigeni and G. F. Giudice, *Nucl. Phys. B* **313**, 725 (1989); J. R. Ellis and R. A. Flores, *Phys. Lett. B* **263**, 259 (1991); J. Engel, S. Pittel, E. Ormand and P. Vogel, *Phys. Lett. B* **275**, 119 (1992); M. T. Ressell, M. B. Aufderheide, S. D. Bloom, K. Griest, G. J. Mathews and D. A. Resler, *Phys. Rev. D* **48**, 5519 (1993); R. Arnowitt and P. Nath, *Phys. Rev. D* **54**, 2374 (1996) [arXiv:hep-ph/9509260]; R. Arnowitt and P. Nath, *Mod. Phys. Lett. A* **10**, 1257 (1995) [arXiv:hep-ph/9408226]; P. Nath and R. Arnowitt, *Phys. Rev. Lett.*

- 74**, 4592 (1995) [arXiv:hep-ph/9409301]; Phys. Rev. D **52**, 4223 (1995) [arXiv:hep-ph/9502399]; V. A. Bednyakov, H. V. Klapdor-Kleingrothaus and S. Kovalenko, Phys. Rev. D **50**, 7128 (1994) [arXiv:hep-ph/9401262]; Nucl. Phys. B **585**, 124 (2000) [arXiv:hep-ph/0001019]; J. L. Feng, K. T. Matchev and F. Wilczek, Phys. Lett. B **482**, 388 (2000) [arXiv:hep-ph/0004043]. J. R. Ellis, A. Ferstl and K. A. Olive, Phys. Rev. D **63**, 065016 (2001) [arXiv:hep-ph/0007113]; A. Bottino, F. Donato, N. Fornengo and S. Scopel, Phys. Rev. D **63**, 125003 (2001) [arXiv:hep-ph/0010203]; M. E. Gomez and J. D. Vergados, Phys. Lett. B **512**, 252 (2001) [arXiv:hep-ph/0012020]; A. B. Lahanas, D. V. Nanopoulos and V. C. Spanos, Phys. Lett. B **518**, 94 (2001) [arXiv:hep-ph/0107151];
- [23] A. Corsetti and P. Nath, Phys. Rev. D **64**, 125010 (2001) [arXiv:hep-ph/0003186]; M. Drees, Y. G. Kim, T. Kobayashi and M. M. Nojiri, Phys. Rev. D **63**, 115009 (2001) [arXiv:hep-ph/0011359]. E. A. Baltz and P. Gondolo, Phys. Rev. Lett. **86**, 5004 (2001) [arXiv:hep-ph/0102147]. Y. G. Kim and M. M. Nojiri, Prog. Theor. Phys. **106**, 561 (2001) [arXiv:hep-ph/0104258]. J. R. Ellis, A. Ferstl, K. A. Olive and Y. Santoso, arXiv:hep-ph/0302032.
- [24] ISAJET, by H. Baer, F. Paige, S. Protopopescu and X. Tata, hep-ph/0001086.
- [25] D. Pierce, J. Bagger, K. Matchev and R. Zhang, Nucl. Phys. B **491** (1997) 3.
- [26] K. L. Chan, U. Chattopadhyay and P. Nath, Phys. Rev. D **58** (1998) 096004.
- [27] J. Feng, K. Matchev and T. Moroi, Phys. Rev. D **61** (2000) 075005.
- [28] H. Baer and C. Balazs, hep-ph/0303114.
- [29] H. Georgi, in *Proceedings of the American Institute of Physics*, edited by C. Carlson (1974); H. Fritzsch and P. Minkowski, Ann. Phys. **93**, 193 (1975); M. Gell-Mann, P. Ramond and R. Slansky, Rev. Mod. Phys. **50**, 721 (1978). For recent reviews, see R. Mohapatra, hep-ph/9911272 (1999) and S. Raby, in Phys. Rev. D **66**, 010001 (2002).
- [30] H. Baer, M. Diaz, J. Ferrandis and X. Tata, Phys. Rev. D **61** (2000) 111701; H. Baer, M. Brhlik, M. Diaz, J. Ferrandis, P. Mercadante, P. Quintana and X. Tata, Phys. Rev. D **63** (2001) 015007; H. Baer and J. Ferrandis, Phys. Rev. Lett. **87** (2001) 211803; D. Auto, H. Baer, C. Balazs, A. Belyaev, J. Ferrandis and X. Tata, arXiv:hep-ph/0302155.
- [31] R. Dermisek and A. Mafi, SO(10) *grand unification in five dimensions: proton decay and the μ problem*, Phys. Rev. D **65** (2002) 055002 [hep-ph/0108139].
- [32] S. Dimopoulos and F. Wilczek, Print-81-0600 (SANTA BARBARA); B. Grinstein, Nucl. Phys. B **206**, 387 (1982); R. Cahn, I. Hinchliffe, L. Hall, Phys. Lett. B **109**, 126 (1982); A. Masiero *et al.* Phys. Lett. B **115**, 380 (1982); I. Antoniadis *et al.* Phys. Lett. B **194**, 231 (1987); R. Barbieri, G. Dvali and S. Moretti, Phys. Lett. B **312**, 137 (1993); K. S. Babu and S. M. Barr, Phys. Rev. D **48**, 5354 (1993); R. Barbieri *et al.* Nucl. Phys. B **432**, 49 (1994) Z. Berezhiani, Phys. Lett. B **355**, 481 (1995).
- [33] Y. Kawamura, Prog. Theor. Phys. **105**, 999 (2001); G. Altarelli and F. Feruglio, Phys. Lett. B **511**, 257 (2001); L. Hall and Y. Nomura, Phys. Rev. D **64**, 055003 (2001); A. Hebecker and J. March-Russell, Nucl. Phys. B **613**, 3 (2001). A. Kobakhidze, Phys. Lett. B **514**, 131 (2001).
- [34] See for example, T. Goto and T. Nihei, *Effect of RRRR dimension five operator on the proton decay in the minimal SU(5) SUGRA GUT model*, Phys. Rev. D **59** (1999) 115009 [hep-ph/9808255];

- K.S. Babu, J.C. Pati and F. Wilczek, *Fermion masses, neutrino oscillations and proton decay in the light of SUPER-KAMIOKANDE*, *Nucl. Phys. B* **566** (2000) 33 [[hep-ph/9812538](#)];
R. Dermisek, A. Mafi and S. Raby, *SUSY guts under siege: proton decay*, *Phys. Rev. D* **63** (2001) 035001 [[hep-ph/0007213](#)];
H. Murayama and A. Pierce, *Not even decoupling can save minimal supersymmetric SU(5)*, *Phys. Rev. D* **65** (2002) 055009 [[hep-ph/0108104](#)].
- [35] G. Jungman, M. Kamionkowski and K. Griest, *Phys. Rept.* **267**, 195 (1996) [[arXiv:hep-ph/9506380](#)].
- [36] H. L. Lai *et al.* [CTEQ Collaboration], *Eur. Phys. J. C* **12**, 375 (2000) [[arXiv:hep-ph/9903282](#)].
- [37] A. Chamseddine, R. Arnowitt and P. Nath, *Phys. Rev. Lett.* **49** (1982) 970; R. Barbieri, S. Ferrara and C. Savoy, *Phys. Lett. B* **119** (1982) 343; L. J. Hall, J. Lykken and S. Weinberg, *Phys. Rev. D* **27** (1983) 2359.
- [38] Joint HEP2 Supersymmetry Working Group, *Combined Chargino Results, up to 208 GeV*, http://alephwww.cern.ch/lepsusy/www/inos_moriond01/charginos.pub.html.
- [39] Joint HEP2 Supersymmetry Working Group, *Combined LEP Selectron/Smuon/Stau Results, 183-208 GeV*, http://alephwww.cern.ch/~ganis/SUSYWG/SLEP/sleptons_2k01.html.
- [40] LEP Higgs Working Group Collaboration, [hep-ex/0107030](#).
- [41] H. Baer, C. Balázs and A. Belyaev, *J. High Energy Phys.* **0203** (2002) 042 and [hep-ph/0211213](#).
- [42] CompHEP v.33.23, by A. Pukhov *et al.*, [hep-ph/9908288](#).
- [43] P. Gondolo and G. Gelmini, *Nucl. Phys. B* **360** (1991) 145; J. Edsjö and P. Gondolo, *Phys. Rev. D* **56** (1997) 1879.
- [44] K. Abe *et al.* (Belle Collaboration), *Phys. Lett. B* **511** (2001) 151.
- [45] D. Cronin-Hennessy *et al.* (Cleo Collaboration), *Phys. Rev. Lett.* **87** (2001) 251808.
- [46] R. Barate *et al.* (Aleph Collaboration), *Phys. Lett. B* **429** (1998) 169.
- [47] H. Baer, C. Balazs, A. Belyaev, J. K. Mizukoshi, X. Tata and Y. Wang, [arXiv:hep-ph/0210441](#); H. Baer, C. Balazs, A. Belyaev, J. K. Mizukoshi, X. Tata and Y. Wang, *JHEP* **0207**, 050 (2002) [[arXiv:hep-ph/0205325](#)].
- [48] H. Baer and M. Brhlik, *Phys. Rev. D* **55** (1997) 3201; H. Baer, M. Brhlik, D. Castaño and X. Tata, *Phys. Rev. D* **58** (1998) 015007.
- [49] G. W. Bennett *et al.* [Muon g-2 Collaboration], *Phys. Rev. Lett.* **89**, 101804 (2002) [Erratum-*ibid.* **89**, 129903 (2002)].
- [50] K. Melnikov, *Int. J. Mod. Phys. A* **16** (2001) 4591 (His updated analysis of the SM value of δa_μ was presented at the High Energy Physics Seminar, University of Hawaii, March 2002); F. Jegerlehner, [hep-ph/0104304](#); K. Hagiwara, A. D. Martin, D. Nomura and T. Teubner, [hep-ph/0209187](#).
- [51] H. Baer, C. Balázs, J. Ferrandis and X. Tata, *Phys. Rev. D* **64** (2001) 035004.
- [52] F. Abe *et al.*, (CDF Collaboration), *Phys. Rev. D* **57** (1998) 3811.

- [53] J. K. Mizukoshi, X. Tata and Y. Wang, *Phys. Rev. D* **66**, 115003 (2002) [arXiv:hep-ph/0208078].
- [54] J. Ellis, T. Falk and K. Olive, *Phys. Lett. B* **444** (1998) 367; J. Ellis, T. Falk, K. Olive and M. Srednicki, *Astropart. Phys.* **13** (2000) 181.
- [55] J. Ellis and K. Olive, *Phys. Lett. B* **514** (2002) 114.
- [56] J. L. Feng, K. T. Matchev and F. Wilczek in [22]
- [57] H. Baer, C. Balazs, A. Belyaev, T. Krupovnickas and X. Tata, hep-ph/0304303.
- [58] For a review, see W. Buchmüller, [arXiv:hep-ph/0204288].
- [59] T. Blazek, R. Dermisek and S. Raby, *Phys. Rev. D* **65** (2002) 115004.
- [60] D. Kaplan, G. Kribs and M. Schmaltz, *Phys. Rev. D* **62** (2000) 035010; Z. Chacko, M. Luty, A. Nelson and E. Ponton, *J. High Energy Phys.* **0001** (2000) 003.
- [61] M. Schmaltz and W. Skiba, *Phys. Rev. D* **62** (2000) 095004 and *Phys. Rev. D* **62** (2000) 095005.
- [62] H. Baer, M. Diaz, P. Quintana and X. Tata, *J. High Energy Phys.* **0004** (2000) 016 and H. Baer, A. Belyaev, T. Krupovnickas and X. Tata, *Phys. Rev. D* **65** (2002) 075024.
- [63] H. Baer, C. Balazs, A. Belyaev, R. Dermisek, A. Mafi and A. Mustafayev, *JHEP* **0205**, 061 (2002) [arXiv:hep-ph/0204108].
- [64] S. M. Barr and I. Dorsner, *Phys. Rev. D* **66**, 065013 (2002) [arXiv:hep-ph/0205088].
- [65] A. Birkedal-Hansen and B. Nelson, *Phys. Rev. D* **64** (2001) 015008 and hep-ph/0211071.